



HAL
open science

Facets of smectic A droplets I. Shape measurements

John Bechhoefer, Lubor Lejcek, Patrick Oswald

► **To cite this version:**

John Bechhoefer, Lubor Lejcek, Patrick Oswald. Facets of smectic A droplets I. Shape measurements. Journal de Physique II, 1992, 2 (1), pp.27-44. 10.1051/jp2:1992111 . jpa-00247610

HAL Id: jpa-00247610

<https://hal.science/jpa-00247610>

Submitted on 4 Feb 2008

HAL is a multi-disciplinary open access archive for the deposit and dissemination of scientific research documents, whether they are published or not. The documents may come from teaching and research institutions in France or abroad, or from public or private research centers.

L'archive ouverte pluridisciplinaire **HAL**, est destinée au dépôt et à la diffusion de documents scientifiques de niveau recherche, publiés ou non, émanant des établissements d'enseignement et de recherche français ou étrangers, des laboratoires publics ou privés.

Classification

Physics Abstracts

68.20 — 61.30E

Facets of smectic A droplets I. Shape measurements

John Bechhoefer(*), Lubor Lejcek(**) and Patrick Oswald

Laboratoire de Physique(***), Ecole Normale Supérieure de Lyon, 69364 Lyon Cedex 07, France

(Received 10 July 1991, accepted 17 October 1991)

Résumé. — Nous avons mesuré des profils de gouttelettes smectique A en fonction de la température pour des matériaux différents. Quand de petites gouttelettes sont refroidies en dessous de la température de transition smectique A-nématique T_{AN} , une facette unique dont le rayon est proportionnel à $(T_{AN} - T)^\alpha$ apparaît. L'exposant α est différent suivant les matériaux mais est compatible avec celui qui est mesuré pour le module de compression des couches B. De plus, nous avons mesuré la forme des régions courbées adjacentes à la facette. Un ajustement avec une loi puissance donne un exposant qui varie avec la température et le matériau et qui, dans tous les cas, est différent de la valeur universelle 3/2. Nous avons aussi étudié comment la forme des gouttelettes relaxe vers l'équilibre et avons trouvé que le temps de relaxation est inférieur à une minute en refroidissant tandis qu'il varie entre quelques heures et quelques jours en chauffant, suivant la valeur de $(T_{AN} - T)$. Une estimation de la barrière d'énergie nécessaire pour nucléer de nouvelles couches suggère que ce processus est interdit et qu'il faut chercher une autre explication à l'asymétrie du taux de relaxation.

Abstract. — We have measured profiles of smectic A droplets in air as a function of temperature for several different materials. When small droplets are cooled below the nematic-smectic A transition temperature T_{AN} , they show a single facet whose radius is proportional to $(T_{AN} - T)^\alpha$. The exponent α differs for different materials but is consistent with that measured for the layer compression modulus B . In addition, we measure the shape of curved regions of the surface adjacent to the facet. A power-law fit gives an exponent that varies with both temperature and material and in any case is different from the universal value of 3/2. We also study how droplet shapes relax to equilibrium and find that while the relaxation time for shape changes upon cooling is less than one minute, that for heating ranges from hours to days, depending on $(T_{AN} - T)$. An estimate of the energy barrier to nucleating new layers suggests that that process is forbidden and that another explanation of the relaxation-rate asymmetry must be found.

(*) *Permanent address:* Dept. of Physics, Simon Fraser University Burnaby, B.C., V5A 1S6, Canada.

(**) *Permanent address:* Institute of Physics, Czechoslovak Academy of Sciences, Na Slovance 2, 18040 Prague 8, Czechoslovakia.

(***) Unité de Recherche Associée 1325 du CNRS.

1. Introduction.

What determines the equilibrium shape of a crystal? A partial answer, given by Wulff and others [1 – 3], is that if one knows the surface energy as a function of orientation with respect to the underlying crystal lattice $\gamma(\theta)$, the shape may be calculated variationally by minimizing the total surface energy while constraining the volume to be constant. The problem then is to model $\gamma(\theta)$. At zero temperature, the equilibrium shape of a crystal consists entirely of facets. As the temperature is raised, thermal fluctuations can wash out a facet *via* the “roughening transition,” which has been intensively studied both experimentally [4] and theoretically [5, 6]. An important point is that facets with different orientations ($\langle 100 \rangle$, $\langle 111 \rangle$, etc.) have different roughening transition temperatures. Thus, typically a crystal at finite temperature will have some orientations that are faceted (atomically flat) and some that are rough (disordered on an atomic scale but smoothly curved on a macroscopic scale).

In this article, we report on experiments whose purpose was to measure the shape of a smectic A liquid crystal in the vicinity of room temperature. Small smectic droplets deposited on a suitably treated glass substrate show round facets on the top of the droplet. These facets are analogous to those found on a crystal and vividly illustrate the solid-like properties of these anisotropic fluids. We shall bring to bear on our observations the theoretical apparatus developed to analyze ideal solid crystals. As in experiments on solids, we shall find that there are many complications peculiar to our own material. Not surprisingly, in our case, the subtleties come ultimately from the fluid-like aspects of liquid crystals.

The rest of this paper is organized as follows: in section 2, we review the predictions of theories describing ideal crystal shapes. In section 3, we discuss the experiment itself. In section 4, we discuss the shape measurements, which focus on the size of facets and the shape of adjoining curved regions. In section 5, we study how the droplets come – or do not come – to equilibrium. In the last section, we raise a number of theoretical issues suggested by our observations. Finally, in an accompanying paper, we take up one of these issues: why it is that only small droplets are faceted.

2. The shape of an ideal crystal.

In this section, we summarize the theory of ideal crystal shapes. Such theories focus on “universal” aspects of equilibrium crystals. Two issues of particular interest are the size of facets and the shape of rounded regions adjoining those facets, which can be modeled as a series of steps whose flat parts are parallel to the facet. (see Fig. 1.) Let the step height be a (usually the lattice spacing), the local step separation d , and the local step density $n = 1/d$ then the steps describe a surface whose local orientation θ with respect to the facet is given by $\tan \theta = a/d$. In order for this description of “vicinal” surfaces to make sense, the step width $\xi \ll d$ or, approximately, $\theta \ll a/\xi$.

Let $E(n)$ be the free energy per unit area along the facet. Since $E = \gamma/\cos \theta$ and $n = \tan \theta/a$, knowing $E(n)$ is equivalent to knowing $\gamma(\theta)$ and the crystal shape. As $n \rightarrow 0$, one expects [6, 7]

$$E(n) = \gamma_0 + \beta n + \phi n^3 + O(n^4) . \quad (1)$$

Here, γ_0 is the surface energy of the facet, β the step energy/length, and ϕ the leading term describing step-step interactions. In general, ϕ has both elastic and entropic contributions. The former arise because the stress field due to one step affects that of its neighbors. The latter arise because steps cannot cross: since a greater separation leaves more modes available

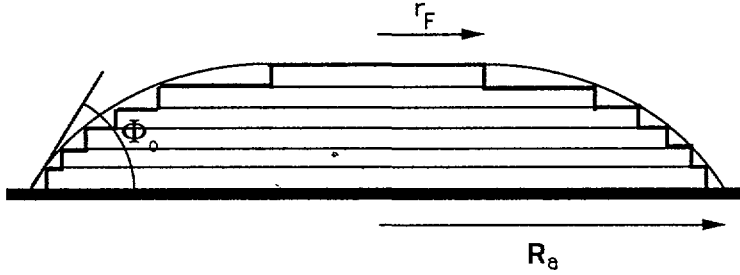


Fig. 1. — View of a smectic A droplet deposited on a flat substrate. If the substrate is treated correctly and the droplet is not too large, then the smectic layers will be flat, the surface will have steps, and the droplet will be faceted.

to fluctuations, entropy produces a step repulsion. There is no $O(n^2)$ term for two reasons: first, the specific models of elasticity and entropic interactions are $O(n^3)$. Second, even if there were $O(n^2)$ terms, they should not be detectable because of thermal fluctuations [7]. More precisely, the facet and the rough orientations can be viewed as distinct thermodynamic phases [8]. Taking $n \rightarrow 0$ is then analogous to approaching a phase transition temperature. If $\phi > 0$ (steps repel each other), then the transition will be second order and the curved part of the crystal will join tangentially onto the facet. The profile $h(r)$ follows a power law

$$h = \begin{cases} 0, & r \leq r_F \\ (r - r_F)^{3/2}, & r > r_F \end{cases} \quad (2)$$

where we consider a round facet of radius $r = r_F$, and h is the height difference between the facet and the crystal surface. For a circular facet, the equilibrium facet radius $r_{F\text{eq}}$ is predicted to be $2\beta/F$, where F is the “supercooling,” which is fixed by the internal hydrostatic pressure of the crystal. More precisely, F represents the work per unit area expended in extending a facet one lattice spacing. Thus, it is equal to the internal hydrostatic pressure times the distance (a) the surface is displaced. $F = 2a\gamma/R$, where γ is the surface energy far from the facet and R is the radius of curvature there. The “shape exponent” $b = 3/2$ in equation (2) is a universal critical exponent, independent of the nature of the solid studied. The $O(n^2)$ term in equation (1) should be undetectable because it is irrelevant in the sense of the renormalization group [7].

Experimental tests of the above theoretical picture have followed three approaches. The first is to use ordinary materials such as lead, gold, or salt. The major difficulty is in establishing thermodynamic equilibrium: the energy barriers that must be broached to reshape a crystal are usually much higher than kT_{melting} and the observed shapes reflect growth rather than conditions. Measurements by Rottman *et al.* [9] on micron-sized crystals suggest that very small crystals do equilibrate and show shapes with exponents consistent with $b = 1.5$; however, Saenz and Garcia [10] analyzed the same data independently and found evidence for a small ($b = 2$) region near the facet. Subsequent measurements by Heyraud and Métois gave $1.6 < b < 2.0$ [11].

The second approach is to study large He^4 crystals, which equilibrate rapidly. Carmi, Lipson, and Polturak [12] found $b = 1.55 \pm 0.06$, but independent measurements by Gallet *et al.* [13] suggest that the experimental errors are larger, probably about 0.2. Also, by measuring the dispersion relation of melting-crystallization capillary waves, Andreeva and Keshishev [14] concluded that d^2E/dn^2 is constant as $n \rightarrow 0$. From equation (1), we see that this implies

an $O(n^2)$ term in $E(n)$. (Two recent – but different! – proposals argue that the quantum nature of helium may resolve the apparent contradiction between capillary wave and shape measurements [15, 16].)

The third approach has been to measure step shapes and separations on silicon wafers directly *via* scanning tunneling microscopy. Although the technique is very promising, the case of silicon is complicated by surface reconstruction, kinks, and the existence of different kinds of steps. The results to date include step-energy measurements [17] and confirmation that on surfaces vicinal to the $\langle 111 \rangle$ face, steps repel each other *via* an elasticity-dominated $O(n^3)$ interaction [18].

In this article, we take a different experimental approach and study the shape of faceted smectic A droplets. Part of the results described here have been summarized in a previous short publication [19]. Although facets on smectic drops have been observed previously [20, 21, 22], ours is the first quantitative study of drop profiles and facet sizes. The smectic A liquid crystal phase consists of stacked two-dimensional fluid layers. One expects a single facet parallel to the layers, so that one avoids the complications that arise when a crystal surface is simultaneously vicinal to two nearby facets [23]. Because the smectic layers are fluid, facets will be round and steps will have no kinks. Also, the transparency, low volatility, and convenient melting point of liquid crystals allow one to do optical experiments in open air near room temperature. Finally, one expects that both the laws describing elastic effects and the way samples relax to equilibrium will be quite different in a smectic as compared to a solid.

3. Experimental methods.

The experimental set up is illustrated in figure 2. A small smectic A droplet (the radius was typically $50 \mu\text{m}$) sits on a glass slide treated with a silane compound (Merck ZLI 2510) to align

layers parallel to the glass (homeotropic orientation). Drops were partially wetting with contact angles ranging from 7° to approximately 20° depending on the materials and fine details of the surface treatment. Contact angle hysteresis was estimated to be a factor of two by measuring the maximum ellipticity of droplets. Only drops round to better than 5% were used.

Detailed experiments were performed on 8OCB, 10OCB, and 4.O.8 [24]. The n OCB series is chemically very stable, allowing a single drop to be used for up to a week with little change in material properties. The major source of impurities was residue from the silane treatment. During the first hour, the nematic-isotropic temperature difference of 8OCB increased from 0.1°C to 0.3°C , where it remained thereafter. By contrast, 4.O.8 contains a Schiff's base and is known to decompose in the presence of oxygen and water vapor. Experiments on 4.O.8 were therefore done quickly, within several hours of the preparation of the sample.

These three materials seem to exhaust the different classes of experimentally observed shapes for thermotropic Sm A droplets. In 8OCB, the phase transition from the smectic A to the nematic phase lying above it in temperature is second order [25]. By contrast, in 10OCB, the smectic A phase undergoes a clear first-order transition to an *isotropic* phase lying above it in temperature. Note that 8OCB and 10OCB differ only in the length of the molecule (10OCB has two extra CH_2 groups).

The material 4.O.8 differs from the previous two in that its molecules have only a very small dipole moment, which is transverse to the long axis of the molecule. As a result, it forms a classic smectic A phase, with a layer spacing equal to the molecular length. [see Fig. 3a.] By contrast, both 8OCB and 10OCB have significant dipole moments lying along the molecules and form "Smectic A_d " phases. In this sub-variety of the smectic A phase, the layer spacing is

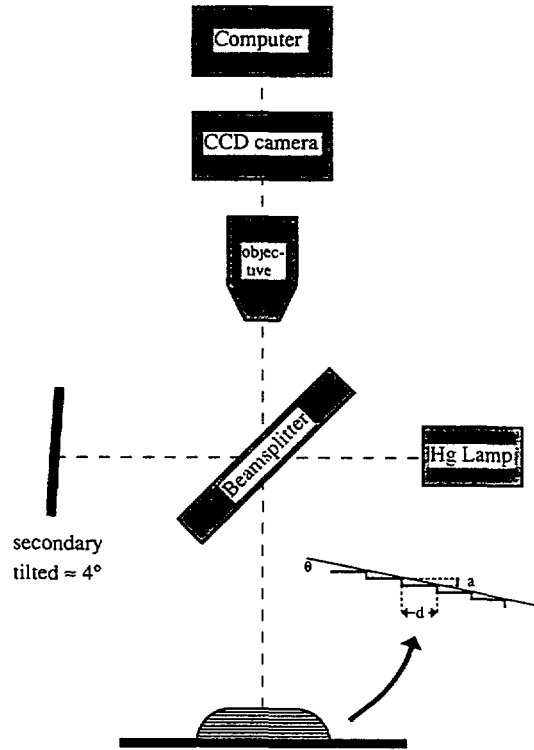


Fig. 2. — Schematic of experimental apparatus, showing liquid-crystal drop and Michelson interferometer.

between one and two times the molecular length, the spacing varying slightly with temperature. In each layer, dipoles are anti-aligned, the “upward-pointing” dipoles slightly displaced relative to the “downward-pointing” dipoles. [see Fig. 3b.]

In addition to the above materials, we also examined briefly AMC_{11} , DOBAMBC, 8CB, and 9.O.4 [26]. All of these materials have smectic A phases that fall into the classification sketched above. (We tested them mainly to examine droplet shapes in phases other than the smectic A phase. The results on other phases are still too sketchy to be discussed here.) We emphasize that for all of the smectics examined, small droplets were faceted.

The droplet shape was measured using a Michelson interferometer (Ealing Electro-Optics 25-0084) combined with detached parts from a Leitz microscope, all mounted to a large, vertical optical rail for greater stability. A microscope objective attached to the beamsplitter of the interferometer projected the image of the fringes onto a CCD camera (Panasonic WV/BL200) and transferred to a Macintosh IIfx computer *via* a frame grabber (Data Translation DT2255). Images were analyzed with the NIH *Image* program [27]. The vertical resolution of the interferometer was enhanced by modulating (by hand) the distance between the droplet and the beamsplitter while tracking the fringe displacement. By recording and quantitatively analyzing multiple images (typically 12 images) of the shifting fringes, we achieved a vertical resolution as good as 20 Å, with 50 Å typical.

One limitation of our interferometer is that light rays impinging on the steeply curved portions of the droplet were deviated so much that they missed the microscope objective.

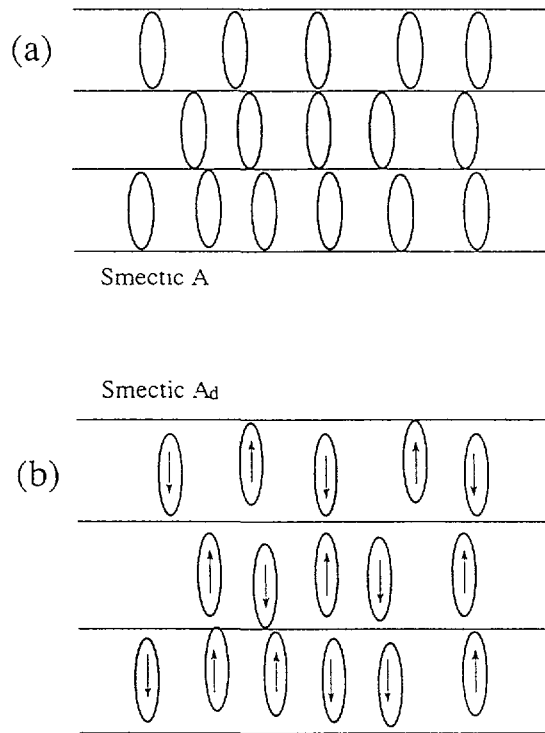


Fig. 3. — Sketch of molecular configuration in two different smectic A configurations. (a) The standard Sm A phase. The layer spacing a equals the molecular length l . (b) The Sm A_d phase. Formed in materials possessing strong dipole moments oriented along the long axis of the molecule, the layered phase has $l > a$.

Thus, the droplet images show fringes only out to 6° inclination, and the outer portion of the droplet appears black (see Fig. 4). For this reason, we were unable to measure accurately either the contact angle or the absolute height of the drop.

Systematic errors were evaluated by imaging isotropic drops and fitting to arcs of a circle. Since we had access only to about 12° , we found that a parabola fit the isotropic profiles equally well. Because results were very sensitive to focusing errors, the focus was checked to $\pm 1 \mu\text{m}$ for each profile by measuring the apparent drop contact-line thickness in white light. In order to locate more precisely the facet edge, we tilted the secondary mirror approximately 4° , thereby increasing the number of fringes lying on the facet. Thus, in the photographs of fringes in figure 4, the glass substrate surrounding the droplet is ruled with vertical fringes from the tilted secondary. In figures 4b-d, the facet may be seen directly since the fringes there are straight, parallel, and spaced the same distance as are the background fringes on the substrate. Another way to see the advantage of tilting the secondary is to compare the technique to heterodyne detection [28]. In both cases, a low-frequency signal is detected by mixing the base signal with a high-frequency carrier wave, which here is the background fringe pattern on the glass plate. After measuring the slope variation around this reference, the signal is "demodulated" by subtracting the known background slope. In this manner, the noise inherent in low-frequency measurements is reduced.

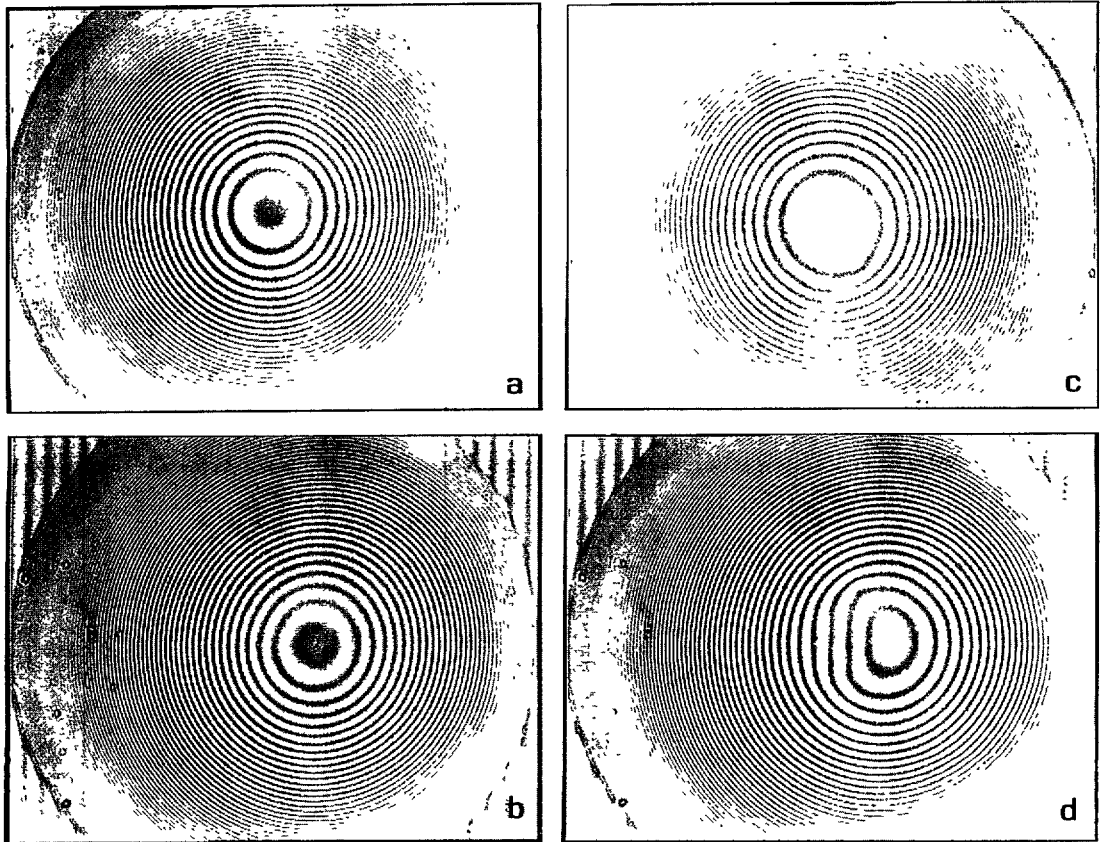


Fig. 4. — Video images of the fringe pattern on a droplet of 4.O.8, as the temperature is lowered. The straight, parallel fringes surrounding the droplet result from a deliberately tilted secondary mirror. The fringes give a contour map with $\lambda/2 \approx 273$ nm separating each fringe. Photos (a) and (b) are of droplets in the nematic phase. Photos (c) and (d) are in the smectic phase. Photo (d) is at $\Delta T = T_{AN} - T = 10^\circ$ C. In (a) and (c) the secondary mirror is exactly perpendicular to the glass substrate of the sample. In (b) and (d), it is slightly inclined from 90° .

4. Profile measurements.

In figure 5, we show the typical evolution of the shape of a small droplet of 8OCB as the temperature is lowered from the nematic phase. Notice the formation of a flat region (facet) below T_{AN} , the nematic-smectic A transition temperature. Droplets whose radius was larger than 100 to 200 μm , depending on the material, were not faceted. See below for a discussion of these size effects. The facet size r_F and the surrounding curved profile adjusts to temperature changes in a time that is shorter than that needed by the oven to change temperatures and restabilize at the new setpoint (about one minute). The only further change observed is a 5% decrease in apparent drop size over several days that we attribute to a change in over-all surface tension due to impurities. Thus, we considered the droplets to be in equilibrium. Below, we discuss this assumption in more detail. The profiles were analyzed by first aligning the facet with the x -axis, with the same rotation being used for all profiles of the same drop. Although

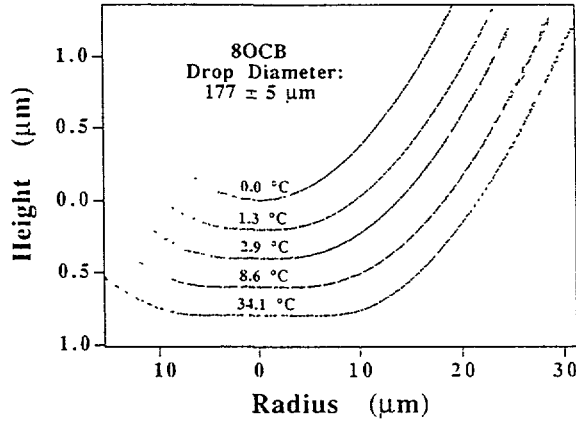


Fig. 5. — Profiles of 8OCB as a function of temperature. The indicated temperatures are the number of degrees centigrade below T_{AN} .

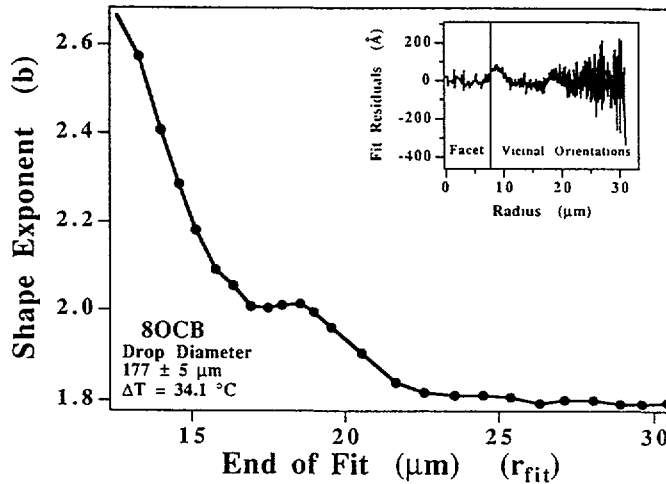


Fig. 6. — The shape exponent b for 8OCB as deduced from fits to equation (3), as a function of the maximum radius of the drop fitted. Inset: the difference between measured values of $h(r)$ and best least-squares fit for $r_{fit} = 30.4 \mu\text{m}$.

independent measurements of the orientation of the facet agreed with that of the glass plate to 10^{-3} radians, we found that accurate curve fits required that the facet be aligned with the x -axis to 10^{-4} radians and thus used the latter as our reference orientation. Once oriented, the height of the facet (the highest point of the curved droplet) was set to zero by hand and the profile was fit to the functional form

$$h = \begin{cases} 0, & r \leq r_F \\ a(r - r_F)^b, & r > r_F \end{cases} \quad (3)$$

with a , r_F and b free parameters. Since one expects that far from the facet $O(n^4)$ terms will become important, we anticipate that equation (3) will hold only out to some unknown value

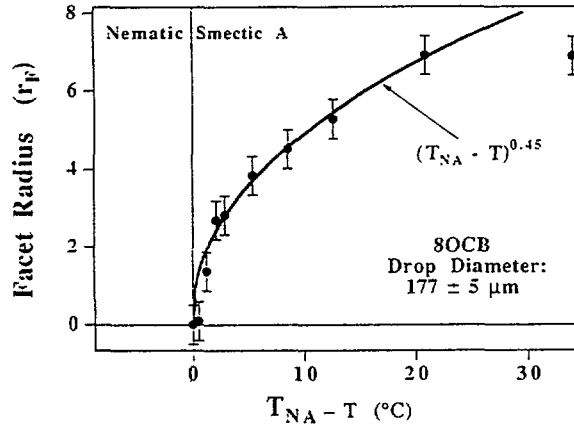


Fig. 7. — Facet size as a function of the temperature below T_{AN} for 8OCB.

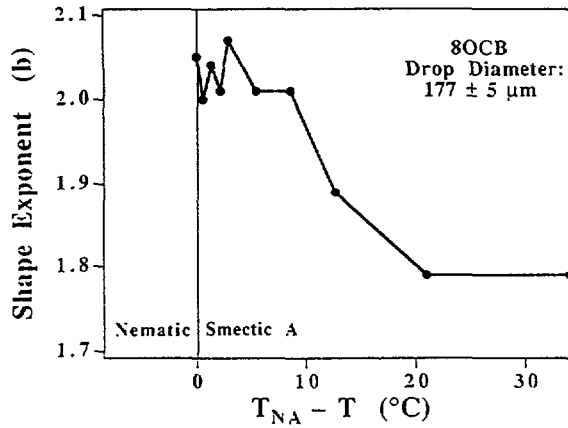


Fig. 8. — Shape exponent b vs. the temperature below T_{AN} for 8OCB.

of $r = r_{fit}$. We thus performed a series of fits to equation (3), tracking parameter values as a function of r_{fit} . As $r_{fit} \rightarrow r_F$, one can show that measurement noise will increase b and decrease r_F . Far enough away from r_F , there was usually a region where the fit parameters were relatively stable, and we used values obtained there. Measurements of 4.0.8 drops showed a tendency for b to rise towards 2 for r_{fit} large enough. We note that this is consistent with the step free energy in equation (1), once higher-order terms ($O(n^4)$ and above) are included in the expansion of $E(n)$. An example of the dependence of b on r_{fit} is given in figure 6a, where there is a stable region from $r_{fit} = 23$ to $30 \mu m$. As figure 6b shows, the resulting fit is good. The major difficulty in these fits is the large sensitivity of b to variations of r_F . While the latter is determined to $\pm 0.5 \mu m$, no matter how the fit is done, the former can vary by ± 0.2 under the same conditions.

As we lower the temperature below the second-order transition at T_{AN} , the facet size grows smoothly from zero and follows a power law $r_F \propto (T_{AN} - T)^\alpha$. By least squares, we fit $\alpha = 0.45 \pm 0.1$ over some $20 \text{ }^{\circ}C$. below T_{AN} for 8OCB (see Fig. 7). The precision in measuring α

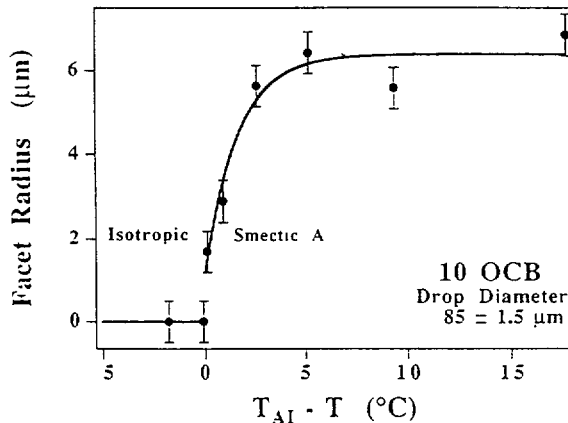


Fig. 9. — Facet size as a function of the temperature below T_{AI} for 10OCB. The jump in facet size at the transition is clearly visible.

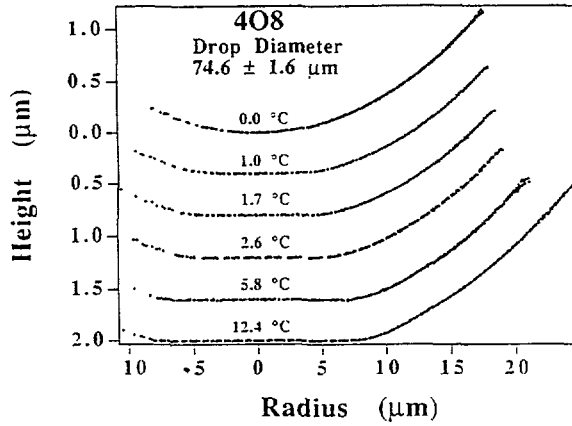
is limited by the uncertainty in determining the facet edge ($\pm 0.5 \mu\text{m}$), in fixing T_{AN} ($\pm 0.1^\circ\text{C}$), and in establishing the minimum and maximum cutoffs in the fit temperatures. Since the nematic-smectic A transition in 8OCB is second order (or very nearly so), a power law implies that r_F is a function of the smectic order parameter. Given that the lack of positional ordering in the nematic phase precludes facets, the above conclusion is not surprising.

The evolution of b with temperature for 8OCB is shown in figure 8. While b decreases from 2 with temperature, it never attains the predicted $3/2$, even some 34°C below T_{AN} . (This is a supercooling of 20°C below crystal-smectic A coexistence.)

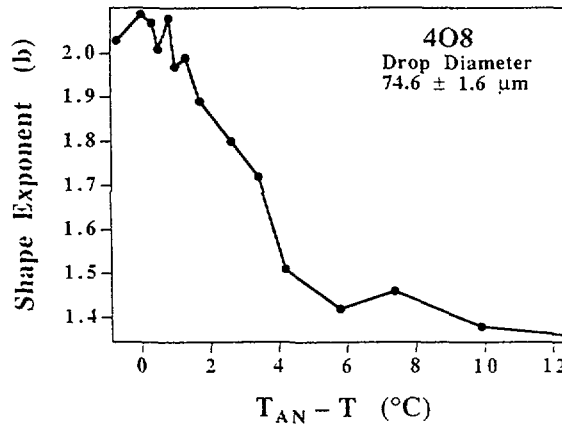
In 10OCB, where the smectic A-isotropic transition is first order, we find that the facet has finite size at the AI transition. (See Fig.9.) This finding also suggests that the facet size is proportional to the smectic order parameter.

For 4.O.8, the behavior was quite different, in that the shape exponent decreased continuously with temperature until the smectic B phase was reached. In small drops (less than about $100 \mu\text{m}$ in diameter), the minimum value of b lay between 1 and 2. (see Fig. 10.) In larger drops, the value fell to one, which meant that a secondary facet had formed around the primary one (see Fig. 11). A graph of facet size *vs.* temperature is shown for the two drops in figures 10c and 11c. We find that in this case, $\alpha = 0.65 \pm 0.1$, over about 4°C .

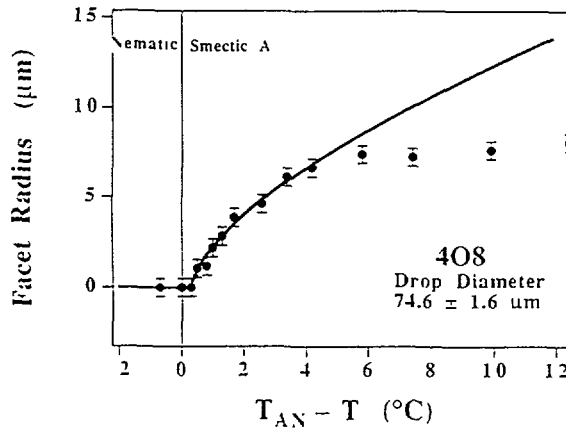
The formation of a secondary facet at low temperatures is unexpected since there is no lattice periodicity along the new facet direction. We note, however, that this facet appears just above the smectic B-smectic A transition temperature of $4.0.8$. Once in the Sm B phase, we observed (as has been noted before by Warengem [29]) many secondary facets that were locally parallel to the droplet surface. Presumably the smectic layers are also locally parallel to the surface. What we see in the Sm A phase near the transition, then, is perhaps a precursor to the behavior observed in the Sm B phase. In any case, we emphasize that in all the drops observed, there was no tendency for $b = 1.5$ to be singled out from other values.



a)

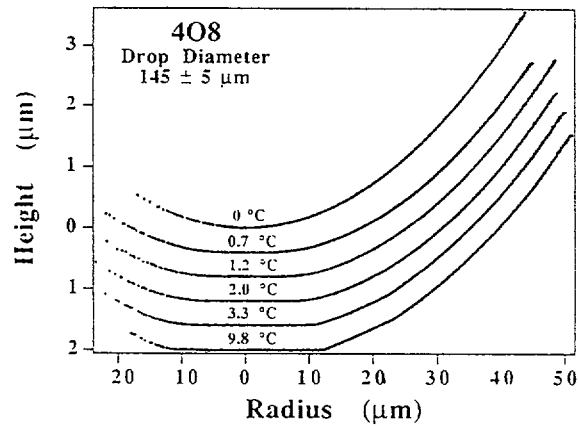


b)

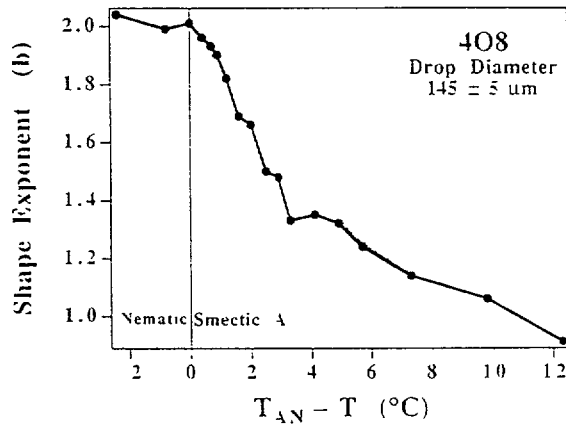


c)

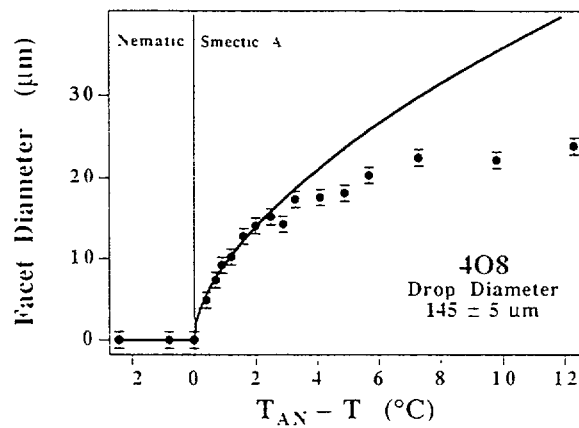
Fig. 10. — (a) Profiles of 4O8 obtained from a droplet whose apparent radius $R_a = 37.3 \mu\text{m}$. The temperatures indicated are the number of degrees below T_{AN} . (b) Shape exponent *vs.* $(T_{AN} - T)$. (c) Facet size *vs.* $(T_{AN} - T)$.



a)



b)



c)

Fig. 11. — Same as figure 10 for a droplet whose apparent radius $R_a = 72.5 \mu\text{m}$. (a) Droplet profiles for different temperatures below T_{AN} . (b) Shape exponent vs. $(T_{AN} - T)$. (c) Facet size vs. $(T_{AN} - T)$.

5. Relaxation to equilibrium.

Among the many reasons for a deviation from the predicted shapes of equilibrium crystals, the most obvious is that the droplets are not in fact in thermodynamic equilibrium. As mentioned above, the relaxation upon cooling is very fast (less than one minute). By contrast, when we raise the temperature from deep within the smectic A phase to just below T_{AN} , the facet shrinks to its former size extremely slowly – on a timescale of hours or even days (see Fig. 12). As $T \rightarrow T_{AN}$, the relaxation time is shorter, although always several orders of magnitude greater than the time necessary to grow facets.

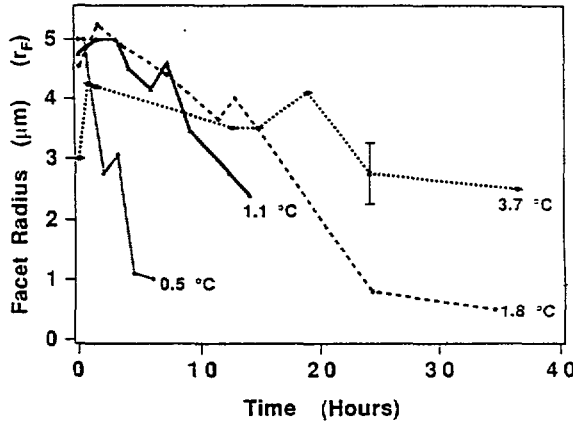


Fig. 12. — Facet size *vs.* time for 8OCB, as a large facet relaxes towards its equilibrium size, for different temperatures. From [19].

An explanation of the relaxation-rate asymmetry is that growing a facet involves removing smectic layers (i.e., making the drop thinner). The timescale τ_p is then set by permeation [30], where a pressure gradient across layers induces a corresponding flow of molecules. It may be estimated as follows: The line tension β of the innermost step (whose radius is r) produces an inward force β/r that tends to shrink the topmost terrace. Molecules in this terrace are at a higher pressure and will permeate down to the next layer. The frictional force fixing the flux of molecules is $a/m(dr/dt)$, where $m \approx \sqrt{\lambda_p/\eta}$ is the mobility of edge dislocations, λ_p is the permeation constant, and η the viscosity. Equating these two forces, we have

$$\frac{a}{m} \dot{r} + \frac{\beta}{r} = 0 \quad (4)$$

Integrating this gives

$$\tau_p = -\frac{a}{\beta m} \int_{r_F}^0 r dr = +\frac{ar_F^2}{2\beta m} \quad (5)$$

Taking $a = 30 \text{ \AA}$, $r_F = 10^{-3} \text{ cm}$, $\beta = 2 \times 10^{-6} \text{ ergs/cm}$ (see below), $\eta = 1 \text{ poise}$, and $\lambda_p = 2 \times 10^{-13} \text{ cgs}$ [31, 32], we find $\tau_p \approx 0.2 \text{ sec}$. This is consistent with the fast relaxation observed upon cooling. By contrast, heating would imply that additional layers must be created *via* two-dimensional nucleation of a small circular germ exceeding a critical radius

r_c . If the energy barrier E_c were greater than kT , the basic relaxation time would be set by $\tau_n = \tau_p e^{E_c/kT}$, thus explaining the relaxation-rate asymmetry. Since the energy barrier could be expected to go to zero as $T \rightarrow T_{AN}$, this would also be consistent with the observed temperature dependence of the relaxation rate.

One test of this scenario would be to see whether the droplet radius stabilizes at a radius r_F upon being warmed. More precisely, assume that we start from T_{AN} and lower the temperature to T_1 . By the argument above, the facet radius will be frozen at $r_c(T_1)$. Continue cooling the droplet to T_2 , which is cold enough so that $r_c(T_2) > 2r_c(T_1)$. Now reheat back up to T_1 . The facet should stabilize at $r_F(T_1) = 2r_c(T_1)$. Unfortunately, our current data are not sufficiently precise to allow such a test.

Although the above explanation is qualitatively satisfactory, there is a snag: the estimated energy barrier is so much bigger than kT that the probability to nucleate a new layer should be essentially zero. To see this, we note that the free energy $E(r)$ of a germ of radius r is [6]

$$E(r) = -\pi r^2 F + 2\pi r \beta \quad (6)$$

Taking $dE/dr = 0$ gives a critical radius $r_c = \beta/F$ and an energy barrier $E_c = \pi\beta^2/F = \pi r_c^2 F$. As mentioned above, we can take $F = 2a\gamma/R$. Assuming that the observed facet radius $r_F \approx r_c$, we have $E_c \approx 2\pi\gamma r_F^2(a/R)$. For 8OCB, near T_{AN} , $r_F = 2 \mu\text{m}$, $\gamma = 30 \text{ erg/cm}^2$, and $R = 100 \mu\text{m}$, we have $E_c \approx 2.3 \times 10^{-10} \text{ erg} \approx 10^4 kT$.

If nucleation of additional layers is forbidden, then another explanation must be found for the observed slow relaxation. Assuming the drop height and volume to be fixed, a change in facet size implies a change in the shape of the round part, or a change in apparent drop radius or contact angle. Experimentally, the drop radius remains constant to better than 0.5% as the facet goes from zero to $7 \mu\text{m}$ and relaxes back to $1 \mu\text{m}$; however, we cannot now rule out a small change in drop height or contact angle.

Another implication of a large barrier height is that since $r_c = 1/2(r_F)_{\text{eq}}$, we expect to observe $r_F \approx r_c$, rather than $r_F = (r_F)_{\text{eq}}$. After a temperature quench, layers whose radius is less than the new r_c will collapse rapidly, on a timescale of τ_p . Once the facet has grown to r_c , removing additional layers requires crossing an energy barrier $E(r)$. Since the scale of this barrier is set by $E(r_c)$, the facet will be frozen at a value just larger than r_c .

If we assume that $r_F \approx r_c$ and not $(r_F)_{\text{eq}}$, we find that, close to the facet edge, the profile of this metastable configuration should have $h(r) \propto (r - r_F)^2$, in agreement with our measurements. To see this, we consider the forces lying on a step. The supercooling F pushes it out. Steps lying beyond the facet edge push it in with a force equal to minus the gradient of the step "chemical potential" $\xi = dE/dn$ [6]. There is also an inward force due to the line tension, $-\xi/r$, where r is the local step curvature radius. Equating these gives

$$F = \frac{\xi}{r} + \frac{d\xi}{dr} \quad (7)$$

Integrating, we have

$$\xi = \frac{Fr}{2} + \frac{A}{r} = \beta + 3\phi \left(\frac{1}{a} \frac{dh(r)}{dr} \right)^2 \quad (8)$$

where A is an integration constant that is fixed by defining the position of the facet edge. Solving equation (8) for $h(r)$, we have

$$h(r) = a \sqrt{\frac{\beta}{3\phi}} \int_{r_F}^r dr \sqrt{\frac{Fr}{2\beta} + \frac{A}{r\beta} - 1} \quad (9)$$

From equation (8), we note that A may be expressed in terms of r_F as $A = r_F(\beta - \frac{Fr_F}{2})$. The integrand is then

$$I = \sqrt{\frac{Fr}{2\beta} + \frac{r_F}{r\beta} \left(\beta - \frac{Fr_F}{2} \right) - 1} \quad (10)$$

If the facet is at its equilibrium size, then $r_F = 2\beta/F$, which gives a height profile of

$$h(r) = \frac{2}{3} \sqrt{\frac{F}{6 \left(\frac{\phi}{a^2} \right)}} (r - r_F)^{3/2} \quad (11)$$

If the facet radius has anything other than its equilibrium value, then the integrand takes the form $I \approx \sqrt{\text{const} + r}$, whose integral gives an exponent of 2. For example, if $r \approx r_c = \beta/F$, then one can evaluate the integral in equation (9) directly to obtain

$$h(r) = r_F \sqrt{\frac{Fr_F}{6 \left(\frac{\phi}{a^2} \right)}} \left[\frac{4}{3} + \left(\frac{2}{3} \frac{r}{r_F} - 2 \right) \sqrt{\frac{r}{r_F}} \right] \quad (12)$$

The expansion around $r/r_F \approx 1$ then gives

$$h(r) = \frac{1}{2r_F} \sqrt{\frac{Fr_F}{6 \left(\frac{\phi}{a^2} \right)}} (r - r_F)^2 \quad (13)$$

Note that for a general value of A , one can express the integral in equation (9) exactly in terms of elliptic integrals. The above conclusions are then directly verified.

The above result implies that in a circular geometry both the facet and the steps must be in equilibrium to see a shape exponent of 3/2. In previous experiments, it is unclear whether the facet had reached its equilibrium size.

A second inference is that, away from T_{AN} , the observed step energy

$$\beta = r_F F = \frac{2\gamma a r_F}{R} \approx 2 \times 10^{-6} \text{ erg/cm} \quad (14)$$

The corresponding step width

$$\xi \approx \gamma a^2 / \beta \approx a(R / (2r_F)) \approx 4.5a \quad (15)$$

(On the other hand, if $r_F = r_{F_{eq}}$, then $\xi \approx 9a$.) In either case, $r_F \propto \beta$, giving an interesting interpretation to our measurements of facet size *vs.* temperature (Fig. 4). The value of the scaling exponent α is consistent with the scaling index measured for the compression modulus B of smectic layers in 8OCB [33] (the exponent there was 0.49 ± 0.03) and suggests that the step energy β is proportional to B .

6. Conclusions.

In this article, we have described in detail experiments measuring the shape of smectic A liquid crystal droplets. Our observations may be summarized as follows:

(1) If the material studied has a second-order phase transition to a nematic phase, then small droplets show facets whose size grows smoothly from zero as the temperature is decreased below the smectic A-nematic transition. If the material studied has an isotropic phase, then a facet of finite size is formed upon entering the smectic phase. These differences mirror the second- and first-order-nature of the respective bulk phase transitions.

(2) Only small droplets, those whose radius is less than approximately $200\ \mu\text{m}$, show facets. Larger droplets have smoothly rounded tops at all temperatures where the droplets are in the smectic A phase.

(3) Studies of the shape of rounded regions adjacent to facets and attempts to fit such shapes to power laws suggest a further classification of behavior as a function of the detailed structure of the smectic A phase, if we assume that the materials we studied were typical of their class. Materials forming a classic smectic A phase show shape exponents near 2 over nearly the entire temperature range of the smectic. Materials forming the Sm A_d phase show shape exponents that decrease from 2 near the smectic A-nematic transition temperature to 1 near a more ordered phase, such as the smectic B phase. In both cases, we did not see evidence that the value of $3/2$ was in any way singled out, although over a certain range of temperature there were profiles of Sm A_d droplets with exponents near this value. We emphasize again that the measurement is delicate, and despite shape measurements as good or better than other experiments concerning crystal shape, we found that the precise value of an exponent was quite sensitive to details of the fit (such as how far out the fit went) and that in the absence of an independent way of determining the position of the facet edge, estimates of the shape exponent should not be overly trusted. We note that in principle the best way to measure such shapes would be to determine the position of each step directly *via* scanning tunneling microscopy or atomic force microscopy.

(4) We studied how the droplets relax to equilibrium. In all cases, it seems likely that the curved regions (with steps) are in equilibrium. The same is perhaps not true for the facet, however. We observed that upon lowering the temperature from a nematic-smectic A transition, facets grew rapidly and did not afterwards change size. But when the temperature was raised back toward the nematic, the facet size shrunk much more slowly, taking hours or even days, depending on the final temperature in relation to T_{AN} .

(5) We also measured the absolute sizes of facets as a function of temperature. Using theoretical predictions that the size should be proportional to the step line tension, we deduce a typical value of 10^{-6} erg/cm for the latter. The exact value for different materials is uncertain, since the proportionality constant depends on the ratio between the actual facet size and the equilibrium facet size, a number for which the uncertainty is at least a factor of two (pending a better model of the smectic orientations in the droplet).

(6) There are a number of observations suggesting that bulk edge dislocations may be present in some of the droplets. In the optical microscope, faint lines are often observed. Second, the occasional facets show a slight rounding (several hundred angstroms over distances of several microns). These observations suggest that the dislocations might be metastable configurations.

These observations raise a number of theoretical issues, only a few of which were touched on in this article. The asymmetric relaxation of facets together with an estimate of the energy barrier to nucleating new smectic layers suggest that the facet size is blocked very close to r_c , which is only half its equilibrium value. We then showed that a blocked facet would lead to a finite-size correction to the predicted $3/2$ scaling law whose leading term had an exponent of

2. While this scenario is consistent for our observations in 8OCB and related Sm A_d phases, it does not match very well with our observations of 4.O.8 and other classic smectics.

Another problem is to explain the asymmetry in facet relaxation rates. As explained above, two-dimensional nucleation of layers, while giving qualitatively the correct behavior seems to lead to quantitative predictions violently in disagreement with experiment: the energy barrier we estimate is some 10,000 kT , which gives essentially infinite nucleation times. One explanation we have not yet considered is the role of volume defects such as screw dislocations and Frank-Read sources [6]. The former are not likely to be of help since a screw dislocation on the facet ought to wind in one direction at roughly the rate it winds in the other direction. Thus, there would be no asymmetry, although the dynamics might be fast in both directions.

An intriguing possibility raised by Nozières [34] is that surface melting may be present on the rough orientations of the smectic, even if the facet remains entirely in the smectic A phase. In this view, the rounded parts of the droplet would be covered with a thin layer of nematic, whose thickness would grow and possibly diverge as the nematic transition were approached. The view is in analogy to surface melting in solid-liquid-vapor systems, where the solid-vapor interface of a crystal becomes covered with a thin liquid layer as the triple point is approached. As has been seen experimentally in lead [35] and discussed theoretically [36], there may be surface melting on the rough orientations but not on a neighboring facet. The theory for such an effect in smectics has not yet been worked out.

Finally, the existence of a critical droplet radius beyond which the droplet is no longer faceted suggests a competition between a configuration in which layers are parallel to the substrate and steps adorn the droplet's surface and one in which layers are rounded and include bulk edge dislocations to meet the substrate boundary condition. (The first layer must be flat.) A detailed consideration of the energies of the two configurations is given in the accompanying article.

Acknowledgements.

We are indebted to P. Nozières and B. Castaing for helpful discussions and thank also M. Kléman for lending us the interferometer. This work was supported by the Centre National de la Recherche Scientifique and the Centre National d'Etudes Spatiales. L. L. acknowledges support from the Chaire Louis Néel and the Région Rhône-Alpes.

References

- [1] Wulff G., *Z. Kristallogr.* **34** (1901) 449.
- [2] Landau L.D., Lifshitz E.M., *Statistical Physics* (Oxford: Pergamon Press, 1980), 3rd Ed. revised by E. M. Lifshitz and L. P. Pitaevskii Part I pp. 520.
- [3] Herring C., in *Structure and Properties of Solid Surfaces*, Ed. by R. Gomer and C. S. Smith (Chicago, Univ. Chicago Press, 1953) pp. 5.
- [4] Wolf P.E., Gallet F., Balibar S., Rolley E., Nozières P., *J. Phys. France* **46** 1987 (1985).
- [5] Chui S.T. and Weeks J.D., *Phys. Rev. B* **14** (1976) 4978.
- [6] Nozières P., *Shape and growth of crystals, to appear in the proceedings of the 1989 Beg-Rohu Summer School* (1991).
- [7] Wortis M., in *Chemistry and Physics of Solid Surfaces VII*, R. Vanselow and R. Howe Eds. (Berlin: Springer Verlag, 1988), pp. 367.

- [8] Andreev A.F., *Sov. Phys. JETP* **53** (1981) 1063.
- [9] Rottman C., Wortis M., Heyraud J.C., Métois J.J., *Phys. Rev. Lett.* **52** (1984) 1009.
- [10] Saenz J.J., Garcia N., *Surf. Sci.* **155** (1985) 24.
- [11] Métois J.J., Heyraud J.C., *Ultramicroscopy* **31** (1989) 73.
- [12] Carmi Y., Lipson S.G., Polturak E., *Phys. Rev. B* **36** (1987) 1894.
- [13] Gallet F., private communication.
- [14] Andreeva O.A., Keshishev K.O., *JETP Lett.* **46** (1987) 200.
- [15] Uwaha M., *J. Phys. France* **51** (1990) 2743.
- [16] Marchenko V. I., Zero steps on a surface of a quantum crystal, preprint.
- [17] Swartzentruber B. S., Mo Y.-W., Kariotis R., Lagally M. G., Webb M. B., *Phys. Rev. Lett.* **65** (1990) 1913.
- [18] Wang X.-S., Goldberg J. L., Bartelt N. C., Einstein T. L., Ellen D. W., *Phys. Rev. Lett.* **65** (1990) 2430.
- [19] Bechhoefer J, Oswald P., *Europhys. Lett.* **15** (1991) 521.
- [20] Bernal J. D., Crowfoot D., *Trans. Faraday Soc.* **29** (1933) 1032.
- [21] Chandrasekhar S., *Mol. Cryst.* **2** (1966) 71.
- [22] Chandrasekhar S., Madhusudana N. V., *Acta Cryst. A* **26** (1970) 153.
- [23] Kashuba A. and Pokrovsky V., *Europhys. Lett.* **10** (1989) 581.
- [24] 8OCB is 4-*n*-octyloxy-4'-cyanobiphenyl; 10OCB is the same chemical with ten CH₂ groups. These chemicals are sold by British Drug House Chemicals, Ltd. 4.O.8 is butyloxybenzilidene octylaniline. We thank J. Malthête for synthesizing it for us.
- [25] It is possible that the AN transition is always at least weakly first order, but any deviations from true second-order behavior would be so small as to be undetectable in our case. For a recent discussion, see Anisimov M. A. *et al.*, *Phys. Rev. A* **41** (1990) 6749.
- [26] AMC11 is 4,4'-undecylazoxymethyl cinnamate, DOBAMBC is decyloxybenzylidene aminomethyl-butyl cinnamate, 8CB is 4,4'-*n*-octylcyanobiphenyl, and 9.O.4 is 4-*n*-nonyloxybenzilidene-4'-*n*-butylaniline.
- [27] NIH "Image" is a public domain program developed by Wayne Rasband, of the National Institutes of Health. Our analysis was done with Version 1.29.
- [28] Steel W. H., *Interferometry*, 2nd Ed., (Cambridge: Cambridge Univ. Press, 1983) pp. 53-54.
- [29] Warenghem, Thèse d'Etat Lille France (1984).
- [30] de Gennes P. G., *The Physics of Liquid Crystals* (Oxford: Oxford University Press, 1975) pp. 310.
- [31] Oswald P., Kléman M., *J. Phys. France* **45** (1984) L-319.
- [32] Oswald P., *J. Phys. France* **48** (1987) 897.
- [33] Ricard L., Prost J., *J. Phys. France* **42** (1981) 861.
- [34] Nozières P., private communication.
- [35] Heyraud J. C., Métois J. J., Bermond J.M., *J. Cryst. Growth* **98** (1989) 355.
- [36] Nozières P., *J. Phys. France* **50** (1989) 2541.